DAC Is Involved in the Accumulation of the Cytochrome b_6/f Complex in Arabidopsis[1][W][OA]

Jianwei Xiao, Jing Li, Min Ouyang, Tao Yun, Baoye He, Daili Ji, Jinfang Ma, Wei Chi, Congming Lu, and Lixin Zhang*

Photosynthesis Research Center, Key Laboratory of Photobiology, Institute of Botany, Chinese Academy of Sciences, Beijing 100093, China

The biogenesis and assembly of photosynthetic multisubunit protein complexes is assisted by a series of nucleus-encoded auxiliary protein factors. In this study, we characterize the *dac* mutant of Arabidopsis (*Arabidopsis thaliana*), which shows a severe defect in the accumulation of the cytochrome b_6/f complex, and provide evidence suggesting that the efficiency of cytochrome b_6/f complex assembly is affected in the mutant. DAC is a thylakoid membrane protein with two predicted transmembrane domains that is conserved from cyanobacteria to vascular plants. Yeast (*Saccharomyces cerevisiae*) two-hybrid and coimmunoprecipitation analyses revealed a specific interaction between DAC and PetD, a subunit of the cytochrome b_6/f complex. However, DAC was found not to be an intrinsic component of the cytochrome b_6/f complex. In vivo chloroplast protein labeling experiments showed that the labeling rates of the PetD and cytochrome *f* proteins were greatly reduced, whereas that of the cytochrome b_6 protein remained normal in the *dac* mutant. DAC appears to be a novel factor involved in the assembly/stabilization of the cytochrome b_6/f complex, possibly through interaction with the PetD protein.

The cytochrome b_6/f (Cyt b6/f) complex is a multisubunit complex that resides in the thylakoid membrane and functions in linear and cyclic electron transport. In the linear process, the complex receives electrons from PSII and transfers them to PSI, a process that is accompanied by the generation of a proton gradient, which is essential for ATP synthesis (Mitchell, 1961; Saraste, 1999). The native form of this complex is present as a dimer with a mass of 310 kD that can be converted into a 140-kD monomer with increasing detergent concentrations (Huang et al., 1994; Breyton et al., 1997; Mosser et al., 1997; Baniulis et al., 2009). In higher plants, the Cyt b6/f monomer contains at least eight subunits: Cyt *f*, Cyt b_6, PetC, PetD, PetM, PetL, PetG, and PetN (Wollman, 2004). PetC and PetM are encoded by nuclear genes, whereas the others are encoded by plastid genes. It has been shown that PetG and PetN are necessary for complex stability in tobacco (*Nicotiana tabacum*; Schwenkert et al., 2007). By contrast, PetL is not required for the accumulation of other subunits of the Cyt b6/f complex, even though it is involved in the stability and formation of the functional dimer (Bendall et al., 1986; Schwenkert et al., 2007). Inactivation of *PetC* in Arabidopsis (*Arabidopsis thaliana*) resulted in significantly reduced amounts of Cyt b6/f subunits and completely blocked linear electron transport, indicating that PetC participates in the formation of the functionally assembled Cyt b6/f complex (Maiwald et al., 2003). In *Synechocystis* sp. PCC 6803, the PetM subunit has no essential role in Cyt b6/f complex electron transfer or accumulation; however, the absence of this subunit apparently affects the levels of other protein complexes involved in energy transduction (Schneider et al., 2001). In addition to the other proteins, FNR was identified as a subunit of the Cyt b6/f complex isolated from spinach (*Spinacia oleracea*) thylakoid membranes (Zhang et al., 2001).

Previous research has revealed how the Cyt b6/f complex assembles into a functional dimer (Bendall et al., 1986; Lemaire et al., 1986; Kuras and Wollman, 1994). In the Cyt b6/f complex, Cyt b_6 and PetD form a mildly protease-resistant subcomplex that serves as a template for the assembly of Cyt *f* and PetG, producing a protease-resistant cytochrome moiety (Wollman, 2004). The PetC and PetL proteins then participate in the assembly of the functional dimer (Schwenkert et al., 2007). PetD becomes more unstable in the absence of Cyt b_6, and the synthesis of Cyt *f* is greatly reduced when either Cyt b_6 or PetD is inactivated, indicating that both Cyt b_6 and PetD are prerequisite for the synthesis of Cyt *f* (Kuras and Wollman, 1994). The reduced synthesis of Cyt *f* can be explained by the so-called CES (for controlled by epistasy of synthesis) mechanism. It is suggested that, in this mechanism, the synthesis rate of some chloroplast-encoded subunits of photosynthetic protein complexes is

[1] This work was supported by the Major State Basic Research Development Program (grant no. 2009CB118500), the Frontier Project of Knowledge Innovation Engineering (grant no. KSCX2–EW–J–1), and the Solar Energy Initiative of the Chinese Academy of Sciences.

* Corresponding author; e-mail zhanglixin@ibcas.ac.cn.

The author responsible for distribution of materials integral to the findings presented in this article in accordance with the policy described in the Instructions for Authors (www.plantphysiol.org) is: Lixin Zhang (zhanglixin@ibcas.ac.cn).

[W] The online version of this article contains Web-only data.

[OA] Open Access articles can be viewed online without a subscription.

www.plantphysiol.org/cgi/doi/10.1104/pp.112.204891

 © 2012 American Society of Plant Biologists. All Rights Reserved.

regulated by the availability of their assembly partners from the same complexes (Choquet et al., 2001). The mechanism of CES for Cyt *f* has been studied in detail in *Chlamydomonas reinhardtii* (Choquet et al., 1998; Choquet and Vallon, 2000). In it, the unassembled Cyt *f* inhibits its own translation through a negative feedback mechanism, and MCA1 and TCA1 have been demonstrated to be involved in the regulation of Cyt *f* synthesis (Boulouis et al., 2011).

Many studies have focused on understanding the conversion of apocytochrome to holocytochrome via the covalent binding of heme in Cyt *f* and Cyt b_6 during the assembly of Cyt b6/f through the CCS and CCB pathways (Nakamoto et al., 2000; Wollman, 2004; de Vitry, 2011). The CCS pathway was originally discovered in the green alga *C. reinhardtii* through genetic studies of *ccs* mutants (for cytochrome *c* synthesis) that display a specific defect in membrane-bound Cyt *f* and soluble Cyt c_6, two thylakoid lumen-resident c-type cytochromes functioning in photosynthesis (Xie and Merchant, 1998). In the CCS pathway, six loci that include plastid *ccsA* and nuclear *CCS1* to *CCS5* have been found in *C. reinhardtii* (Xie and Merchant, 1998). In these mutants, the apocytochrome is normally synthesized, targeted, and processed, but heme attachment is perturbed. The CCB pathway is involved in the covalent attachment of heme c(i) to Cyt b_6 on the stromal side of the thylakoid membranes (Kuras et al., 2007). The *ccb* mutants show defects in the accumulation of subunits of the Cyt b6/f complex and covalent binding of heme to Cyt b_6 (Lyska et al., 2007; Lezhneva et al., 2008). However, heme binding is not a prerequisite for the assembly of Cyt b_6 into the Cyt b6/f complex, although the fully formed Cyt b6/f showed an increased sensitivity to protease (Saint-Marcoux et al., 2009).

The assembly of the Cyt b6/f complex is a multistep process, and current studies have shown that the covalent binding of heme to Cyt *f* and Cyt b_6 is highly regulated. Thus, it is reasonable to speculate that, similar to the other photosynthetic protein complexes (Mulo et al., 2008; Nixon et al., 2010; Rochaix, 2011), the assembly of the Cyt b6/f complex is also assisted by many nucleus-encoded factors. In this study, we characterized an Arabidopsis protein, DAC (for defective accumulation of Cyt b6/f complex), that seems to be involved in the assembly of the Cyt b6/f complex. In addition, we provide evidence that DAC interacts directly with PetD before it assembles within the Cyt b6/f complex.

RESULTS

Identification and Phenotype of the *dac* Mutant

Screening mutants altered in chlorophyll fluorescence has been used to identify nucleus-encoded factors involved in the process of photosynthesis (Meurer et al., 1996; Peng et al., 2006). Proteomic studies of the thylakoid membrane in Arabidopsis have revealed the presence of conserved thylakoid membrane proteins of unknown function (Peltier et al., 2002; Friso et al., 2004). We identified one of these, herein designed DAC, by screening for high chlorophyll fluorescence in a population of T-DNA insertion mutants. The *dac* homozygous plants were unable to grow photoautotrophically in soil (data not shown) and could be maintained on Suc-supplemented medium, but they did not develop any fertile flowers. Additionally, the mutants showed a retarded growth pattern and exhibited pale green leaves under normal growth conditions (Fig. 1A); when grown under low light (20 μmol m^{-2} s^{-1}), the mutant plants were greener and the growth was less affected (data not shown). This insertion mutant line (SALK_088638) carries an insert in the fourth exon of the *DAC* gene (*AT3G17930*; Fig. 1B). In the *dac* mutant, the expression of *AT3G17930* was completely suppressed, as determined by reverse transcription-PCR analysis (Fig. 1C). We next isolated thylakoid membranes and performed an immunoblot analysis using specific anti-DAC, anti-PetD, and anti-LTD (raised against the Light-Harvesting Protein translocation defect in Arabidopsis; Ouyang et al., 2011) antibodies, and the DAC protein was barely detectable (Fig. 1D).

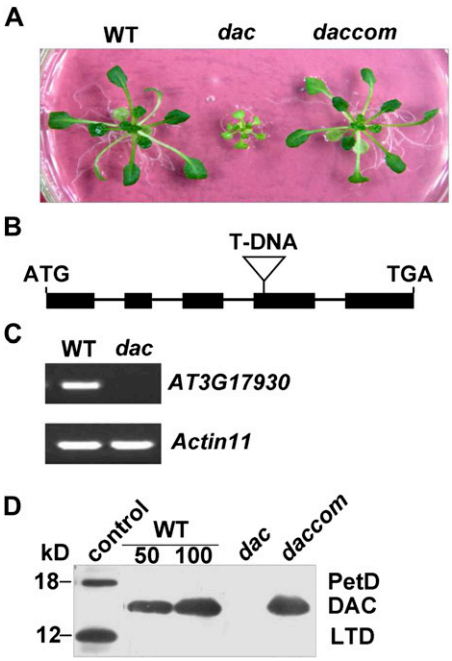

Figure 1. Identification of the *dac* mutant. A, Identification and complementation of the *dac* mutant. The cDNA of the wild-type *DAC* gene was cloned into a binary plant transformation vector and used for complementation of the *dac* mutant (*daccom*). WT, Wild type. Four-week-old plants grown on Suc-supplemented medium are shown. B, Schematic diagram of the *DAC* gene. Exons are indicated by black boxes, introns by lines, and the T-DNA insertion by the triangle; ATG represents the initiation codon and TGA represents the stop codon. C, Reverse transcription-PCR analysis. Reverse transcription-PCR was performed using specific primers for *AT3G17930* or *ACTIN11*. D, Thylakoid membranes (2 μg of chlorophyll) isolated from wild-type and *dac* mutant leaves were separated by Tricine/SDS-PAGE followed by immunoblot analysis with the anti-DAC, anti-PetD, and LTD antibodies. LTD and PetD are used here as molecular mass controls.

Chlorophyll fluorescence induction kinetics analysis showed the ratio of variable to maximum fluorescence, which is customarily used to indicate the maximum potential capacity of PSII. This value is reduced in the *dac* mutant (0.67 ± 0.03) compared with the wild type (0.81 ± 0.02), which indicated that the PSII efficiency is down-regulated in the mutant (Fig. 2A). By contrast, the fraction of the PSII reaction centers remaining in the open state under continuous illumination was drastically reduced in *dac* (0.15 ± 0.02) compared with the wild type (0.88 ± 0.02). This result suggests that electrons accumulated in the plastoquinone pool and, thus, were not transferred downstream of the photosynthetic electron transport chain (Meierhoff et al., 2003), which may be due to a block in the electron transport capacity between the two photosystems or a defect in PSI. We further measured the absorbance kinetics of P700 at 820 to 870 nm to study the redox activity of the PSI reaction center (Fig. 2B; Supplemental Table S2). P700 could be oxidized in the mutant by far-red light, which indicated that PSI was functional in *dac*. Thus, spectroscopic analyses indicated that PSII and PSI were functional in *dac*, even though the electron transport capacity between the two photosystems was perturbed. Complementation of the *dac* mutant with the full-length coding region of *AT3G17930* confirmed that inactivation of the *AT3G17930* gene was responsible for the phenotype of the *dac* mutant (Fig. 1A). The DAC level in the thylakoid membrane fraction of complemented plants was equivalent to that of the wild-type plants, which also confirmed this result (Fig. 1D).

Reduced Content of the Cyt b6/f Complex in the *dac* Mutant

The above results suggested the potential impairment of electron transfer between PSII and PSI in the *dac* plants (Fig. 2). To test this hypothesis, we extracted total protein from wild-type and *dac* leaves and performed an immunoblot analysis using specific antibodies against the major subunits of the thylakoid protein complexes (Fig. 3A). The results showed that the levels of the Cyt b6/f subunits, Cyt *f*, Cyt b_6, PetC, and PetD, were decreased to 10% to 15% of wild-type levels and that the protein contents of D1 and PsbO of PSII were reduced to 50% to 70% of wild-type levels. The amounts of the PSI proteins, PsaA/B and PsaN, were also reduced to approximately 50% of wild-type levels. There were no apparent changes in the β-subunit of ATPase and the 2Fe-2S protein ferredoxin (Fd) in mutant plants (Fig. 3A; Supplemental Fig. S1). When we cultivated the plants in very dim light (20 μmol m^{-2} s^{-1}), the steady-state levels of PSI and PSII recovered to nearly wild-type levels (data not shown), suggesting that the reductions in PSII and PSI may be due to a secondary effect and also indicating that the *dac* mutant is light sensitive. Defects in heme biosynthesis can result in low accumulation of the Cyt b6/f complex (Lennartz et al., 2001; Lezhneva et al., 2008). To test for this, we assayed thylakoid membranes of the wild type and mutants for the presence of Cyt *f* and Cyt b_6 holoproteins by virtue of their heme-associated peroxidase activities. This analysis revealed that heme binding was not perturbed in the *dac* mutant (Fig. 3B).

To examine the state of Cyt b6/f assembly, we performed blue-native (BN)-PAGE to separate the protein complexes from the thylakoid membranes after solubilization with dodecyl β-D-maltoside (DM; Schägger et al., 1994). Mutant and wild-type thylakoids (loaded on the basis of equal amounts of chlorophyll) were separated electrophoretically in the presence of Coomassie blue G250. The constitutive subunits of the protein complexes were then separated in a second dimension using Tricine/SDS-PAGE, and the proteins were immunoblotted using anti-Cyt b_6 and anti-PetD antibodies (Fig. 3C). In the BN-PAGE analysis, longer exposure times were required to detect the bands of dimer and monomer in *dac* compared with wild-type plants, indicating that the subunits of the Cyt b6/f complex were considerably decreased in mutant plants. Moreover, the ratio between the monomer and dimer was lower in the *dac* mutant than in the wild-type plants. Additionally, an increase in the levels of the intermediate relative to the monomer and dimer of Cyt b6/f was observed in *dac* compared with the wild type (Fig. 3C).

Synthesis and Stability of the Cyt b6/f Complex

To address whether the reduced abundance of Cyt b6/f subunits observed in the *dac* mutant was due to reduced levels of the corresponding mRNAs, the transcripts of eight subunits of the Cyt b6/f complex were analyzed by RNA gel-blot hybridization. As show in Figure 4A, the abundance and pattern of transcripts of the subunits of Cyt b6/f examined were unaltered in the mutant.

To investigate whether the reduced accumulation of the Cyt b6/f complex was due to reduced synthesis of its subunits, in vivo pulse-labeling experiments were performed in which young seedlings were pulse labeled with [^{35}S]Met in the presence of cycloheximide, an inhibitor of nucleus-encoded protein synthesis. During the labeling, the synthesis rate and protein stability of newly synthesized proteins can be monitored. After pulse labeling, the labeled subunits of Cyt b6/f could not be identified clearly because the D1 and D2 subunits of PSII were heavily labeled. Thus, immunoprecipitation experiments were performed. After pulse labeling for 10 and 30 min, thylakoid membranes with equal amounts of chlorophyll were isolated, solubilized, and incubated with an excess of specific antibodies raised against Cyt *f*, Cyt b_6, PetD, and CF1β. To ensure that the newly synthesized proteins were immunoprecipitated completely, the supernatants from the first round of immunoprecipitation were subjected to another round of immunoprecipitation (Barkan et al., 1994; Lennartz et al., 2001). As shown in Figure 4B, the rate of labeling of the Cyt b6/f subunits Cyt *f* and PetD was greatly reduced in the *dac* mutant, but the synthesis of Cyt b_6 was not affected

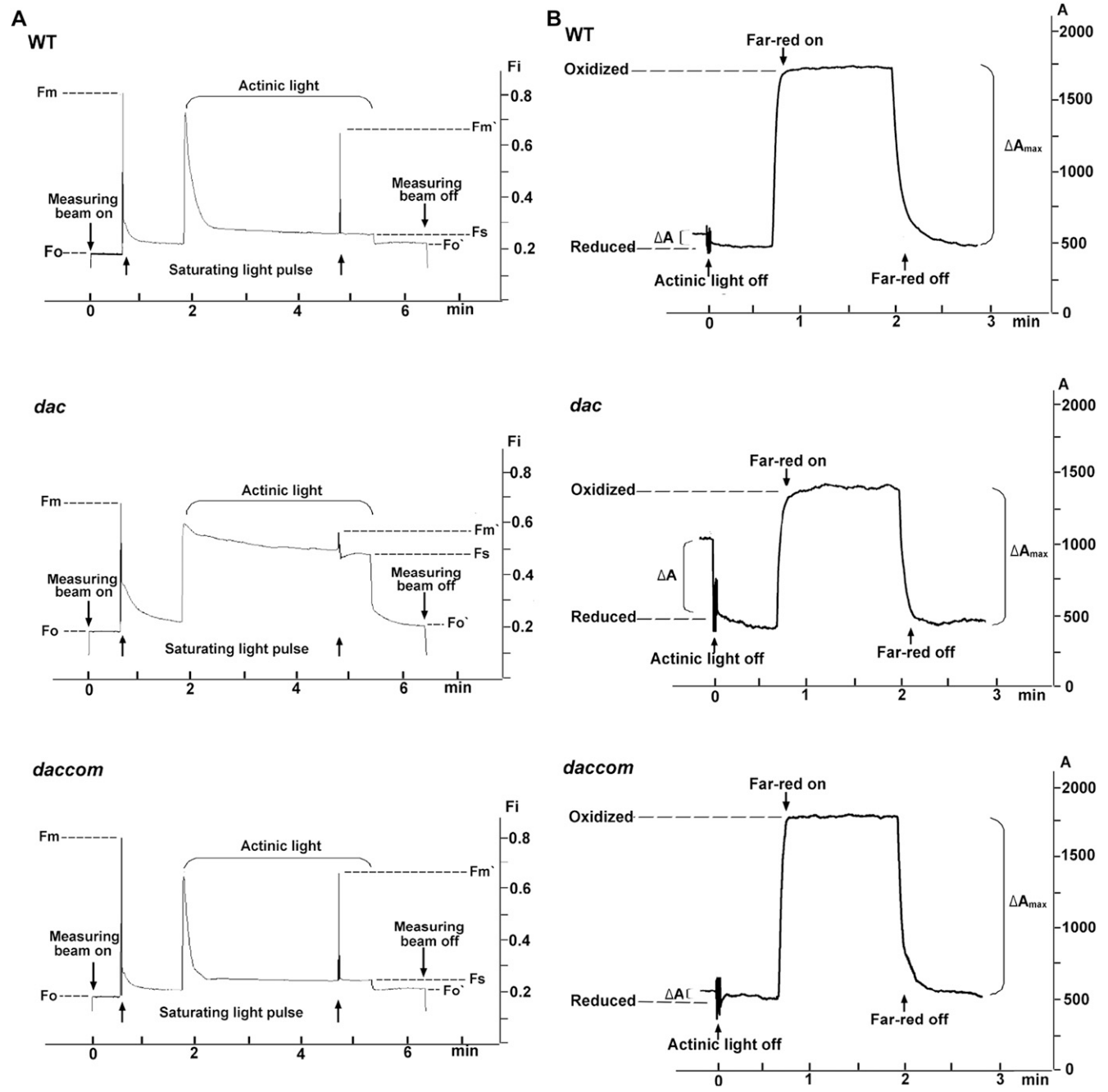

Figure 2. Spectroscopic analyses. A, Chlorophyll fluorescence induction. Fi, Fluorescence intensity; Fm, maximum fluorescence; Fm′, maximum fluorescence under steady-state conditions; Fo, minimal fluorescence; Fo′, minimal fluorescence under a light-adapted state; Fs, steady-state fluorescence; WT, wild type. B, Redox kinetics of P700. A, Relative absorbance; ΔA, oxidation of P700 under actinic light; ΔAmax, maximum oxidation induced by far-red light.

after pulse labeling for 30 min. When the time of pulse labeling was shortened to 10 min, the amount of radioactivity incorporated into Cyt b_6, PetD, and Cyt *f* in the *dac* mutant relative to wild-type levels was increased compared with that after 30 min of labeling.

Altered efficiency of translation initiation can be visualized through analyzing ribosomal loading of specific RNAs. The effects of the *dac* mutation on the translation capacity of the *petA* and *petB*/*petD* transcripts were further examined by analyzing the association of *petA* and *petB*/*petD* transcripts with polysomes. The results showed that the association of these transcripts with polysomes was largely unaffected in the mutant plants (Fig. 5A), which suggested that translation initiation for these transcripts is not affected.

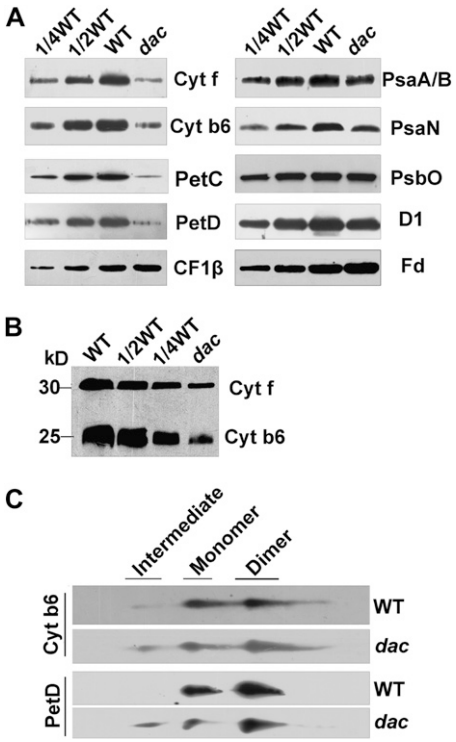

Figure 3. Analysis of chloroplast proteins. A, Immunoblot analysis of chloroplast proteins. Total proteins were separated by 10% Tricine/SDS-PAGE, electroblotted, and probed using specific anti-Cyt *f*, anti-Cyt b_6, anti-PetC, anti-PetD, anti-CF1β, anti-PsaA/B, anti-PsaN, anti-PsbO, anti-D1, and anti-Fd antibodies. WT, Wild type. B, Analysis of the peroxidase activity of the heme-binding proteins Cyt *f* and Cyt b_6. Peroxidase activity was detected by enhanced chemiluminescence. C, BN-SDS-PAGE analysis of thylakoid membrane complexes. Thylakoid membranes (10 μg of chlorophyll) were solubilized with 1% DM and separated on 4.5% to 13.5% acrylamide gradient gels. After the BN gel separation, the excised lanes were soaked in SDS sample buffer and 5% β-mercaptoethanol for 30 min and layered onto 10% Tricine/SDS polyacrylamide gels. After electrophoresis, the resolved proteins were subjected to immunoblot analysis using anti-Cyt b_6 and anti-PetD antibodies. The positions of the Cyt b6/f monomer and dimer are indicated above the image, according to Lennartz et al. (2006).

We also tested the stability of the assembled Cyt b6/f complex in the *dac* mutant with respect to the wild type; the rates of degradation of the Cyt b6/f complex were studied in the presence of lincomycin, an inhibitor of protein synthesis in the chloroplast. Thylakoid membranes were isolated every 2 h from 0 to 8 h after the addition of lincomycin, and immunoblotting was performed for Cyt *f*, Cyt b_6, PetD, D1, and CF1β. As shown in Figure 5B, levels of Cyt *f*, Cyt b_6, and PetD in the *dac* mutant were decreased by the same extent as in the wild type, and about 25% of the D1 protein was degraded in both the wild-type and mutant plants after treatment for 8 h These results indicate that the assembled subunits of Cyt b6/f are fairly stable. By contrast, the newly synthesized proteins displayed very short half-lives in the mutant (Fig. 4B).

DAC Is an Integral Thylakoid Membrane Protein

The *DAC* gene encodes a polypeptide of 190 amino acids with a putative chloroplast transit peptide of 50 amino acids at its N terminus (Fig. 6), as predicted by the TargetP 1.1 and ChloroP 1.1 programs. BLAST searches revealed that the orthologs of DAC contain an uncharacterized domain, DUF3007 (amino acids 87–184; Fig. 6). DAC homologs exist in almost all of the sequenced photosynthetic eukaryotes and cyanobacteria. The most similar homologs were found in *Oryza sativa* (Os01g0805200; 71% identity, 88% similarity), *C. reinhardtii* (58% identity, 77% similarity),

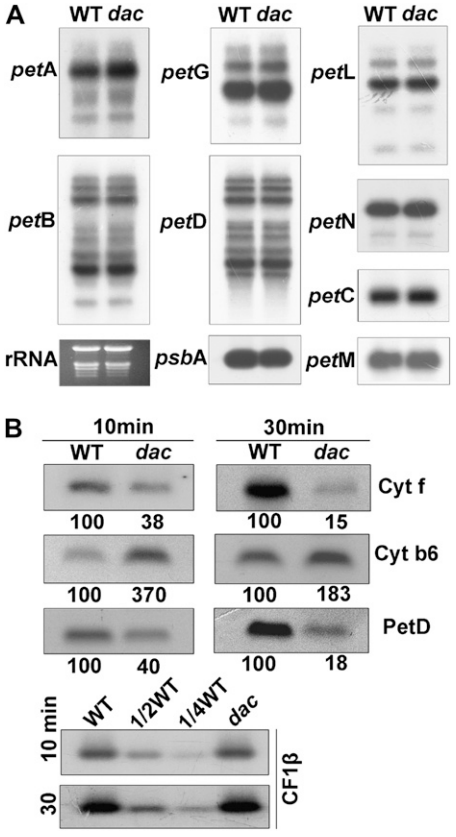

Figure 4. mRNA expression and in vivo protein synthesis in chloroplast. A, RNA gel-blot hybridization with total RNA from the leaves of wild-type (WT) and *dac* plants. Preparations (10 mg) of total leaf RNA from 5-week-old wild-type and *dac* plants were size fractionated by agarose gel electrophoresis, transferred to a nylon membrane, and probed with ^{32}P-labeled cDNA probes for *petA*, *petB*, *petC*, *petD*, *petG*, *petL*, *petM*, *petN*, and *psbA*. Ribosomal RNA was visualized by staining with ethidium bromide as an equal loading control. B, In vivo protein synthesis. Primary leaves of 15-d-old plants were radiolabeled with [^{35}S]Met for 30 min. The thylakoid membranes were solubilized and incubated with anti-Cyt *f*, anti-Cyt b_6, anti-PetD, and anti-CF1β antibodies. The immunoprecipitated samples were separated by Tricine/SDS-PAGE and visualized using autoradiography. X-ray films were scanned and analyzed using an AlphaImager 2200 documentation and analysis system. The protein level percentages shown below the lanes were estimated by comparison with the wild type.

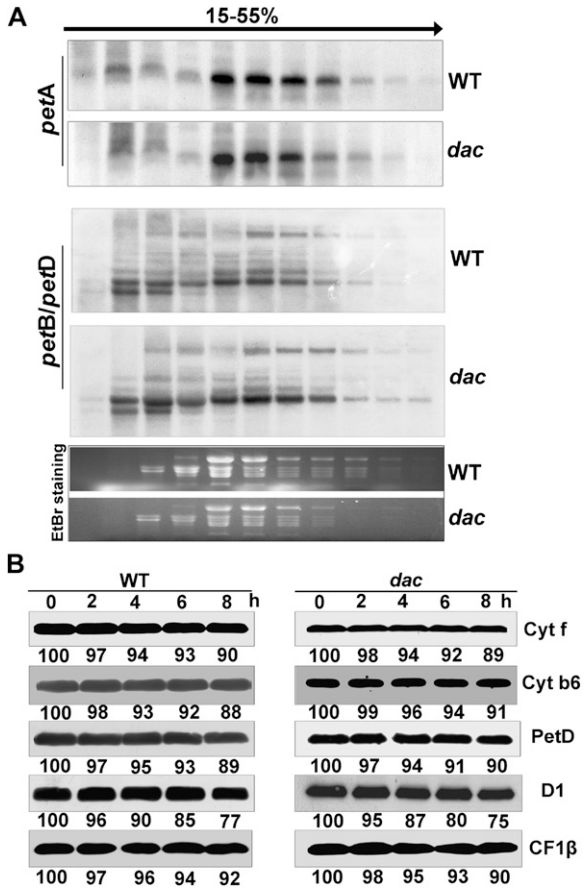

Figure 5. Polysome accumulation and protein stability analysis. A, Association of *petA* and *petB*/*petD* mRNAs with polysomes. Eleven fractions of equal volume were collected from the top to the bottom of 15% to 55% Suc gradients, and equal proportions of the RNA purified from each fraction were analyzed by gel-blot hybridization. Ribosomal RNAs were detected by ethidium bromide staining. B, Stability of the Cyt b6/f complex. Arabidopsis leaves were incubated with lincomycin for 30 min and illuminated for various time periods. After this treatment, the thylakoid membranes were isolated, and their contents of photosynthetic proteins were determined by immunoblot analysis. The protein level percentages shown below the lanes were estimated by comparison with levels found in corresponding samples taken at time zero. WT, Wild type.

and *Synechococcus elongatus* PCC 6301 (49% identity, 64% similarity; Fig. 6). To determine its subcellular localization, we fused the full-length DAC protein to the N terminus of synthetic GFP, and the DAC-GFP fusion protein was transiently expressed in Arabidopsis protoplasts under the control of the cauliflower mosaic virus 35S promoter. The GFP fluorescence signal revealed that the DAC protein was located in the chloroplast (Fig. 7A).

The DAC protein is also predicted to be located in the thylakoid membrane and to possess two transmembrane (TM) domains, according to the TMHMM program (Fig. 6; amino acids 92–114 and 124–146 for DAC). The DAC protein can be detected in thylakoid membranes and could not be extracted from the sonicated thylakoid membranes when incubated with different salts, which was similar to what was observed for the CP47 protein. However, the peripherally associated lumenal protein PsbO was released after this treatment (Fig. 7B), indicating that DAC is an integral thylakoid membrane protein. To determine the topology of DAC more precisely, the thylakoid membranes were digested with trypsin (Sun et al., 2007) and subjected to immunoblot analysis with the DAC antibody, which was raised against the C-terminal hydrophilic portion (43 amino acids in length; Fig. 7C). The N- and C-terminal regions of DAC contain trypsin cleavage sites, but the loop between the TM domains does not. Thus, if the DAC protein could be degraded by trypsin, the N-terminal and C-terminal regions must be located on the stromal side of the thylakoid membrane (as shown in Fig. 7D); otherwise, the topology would be as indicated in Figure 7E. Our results showed that DAC was degraded completely within 15 min in the presence of trypsin; by contrast, the lumenal protein PsbO was not affected (Fig. 7D). Therefore, these results indicate that the N terminus of DAC is located in the chloroplast stroma, as illustrated in Figure 7D.

DAC Interacts with PetD

To examine whether the DAC protein is a component of the Cyt b6/f complex, thylakoid membranes were solubilized with DM and separated by Suc gradient sedimentation, and 20 fractions of equal volume were collected. The proteins in each fraction were separated by Tricine/SDS-PAGE followed by immunoblot analysis using specific antibodies. Based on the migration patterns of the protein fractions, our results indicate that DAC has a mass of 80 to 100 kD (Fig. 8A); the monomer and dimer of Cyt b6/f migrated to positions of approximately 140 and 310 kD, respectively. Thus, although the DAC protein does not comigrate with Cyt b6/f, we cannot exclude the possibility that DAC interacts with the subunits of the Cyt b6/f complex, because the DAC protein overlapped somewhat with the subunits of the Cyt b6/f complex in the Suc gradient fractions.

To study the potential function of DAC, we employed a modified split-ubiquitin system to examine the relationship between DAC and the subunits of Cyt b6/f (Stagljar et al., 1998). Prey plasmids containing the NubG moiety fused to the N terminus of the mature Cyt b6/f subunits and DAC were transformed into the NWY32 strain, in which bait proteins were expressed; the bait plasmid was constructed to generate the fusion protein LexA-VP16-Cub-DAC. The resulting transformants were analyzed for growth on synthetic dextrose (SD) plates lacking His, Leu, Trp, and adenine (SD-His-Leu-Trp-Ade), and their β-galactosidase activity was assayed. As shown in Figure 8B, the coexpression of LexA-VP16-Cub-DAC with NubG-PetD allowed NWY32 to grow on SD-His-Leu-Trp-Ade medium and resulted in positive β-galactosidase activity. These results indicate that DAC interacts

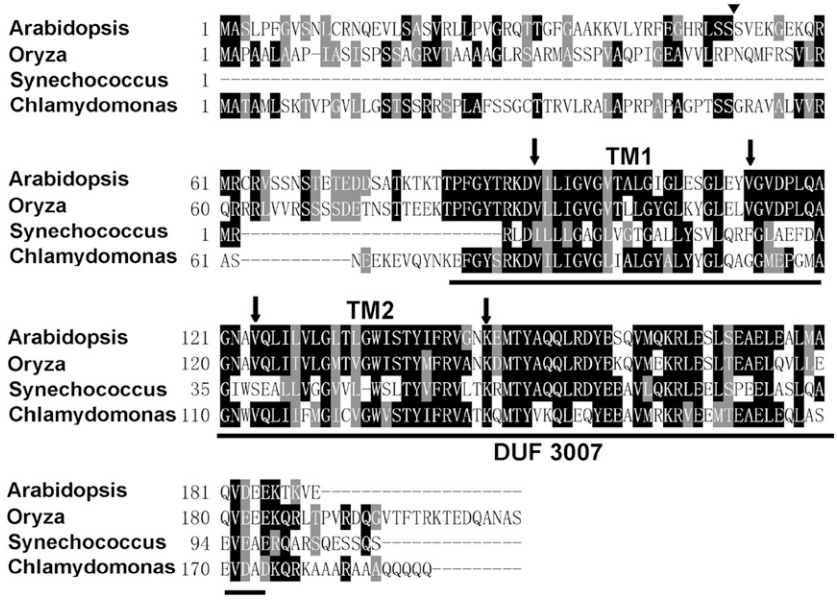

Figure 6. Amino acid sequence alignment of the DAC protein. The amino acid sequence of the Arabidopsis DAC protein (AT3G17930) was compared with homologous sequences from *O. sativa* (Os01g0805200), *C. reinhardtii*, and *S. elongatus* PCC 6301. Black boxes indicate strictly conserved amino acids, and gray boxes indicate closely related residues. The inverted triangle indicates the putative chloroplast transit peptides, and the arrows above the sequences demark the two TM domains (TM1 and TM2). The chloroplast transit peptide was predicted using TargetP 1.1 and ChloroP 1.1, and the TM domains were predicted using the TMHMM program. The black line indicates the DUF3007 domain.

with PetD but not with the other subunits of the Cyt b6/f complex or itself in yeast (*Saccharomyces cerevisiae*).

To study further whether interaction occurs in vivo, DM-solubilized thylakoid membranes were incubated with protein A/G-agarose beads coupled to the anti-DAC antibody, and the coimmunoprecipitated samples were subjected to immunoblot analysis with specific anti-Cyt *f*, anti-Cyt b_6, and anti-PetD antibodies. Our results showed that PetD, but not Cyt b_6 or Cyt *f*, was immunoprecipitated by the anti-DAC antibody (Fig. 8C). These results provide additional evidence for a specific interaction between PetD and DAC.

DISCUSSION

The biogenesis and assembly of the Cyt b6/f complex is a complicated process that is regulated at the levels of transcription, translation, and complex assembly (Bruce and Malkin, 1991; Saint-Marcoux et al., 2009; Boulouis et al., 2011). The synthesis and sequential assembly of the subunits and the binding of various cofactors require a series of additional nucleus-encoded assembly factors (Kuras et al., 1997; Lennartz et al., 2001, 2006). The identification of these factors and the elucidation of their functions will provide new insights into the mechanisms underlying the assembly and maintenance of the Cyt b6/f complex. This study reports the characterization of a previously uncharacterized Arabidopsis protein, DAC, which appears to be involved in the assembly of PetD into the Cyt b6/f complex. Database searches revealed that homologs of the DAC protein are present in organisms containing Cyt b6/f complexes, such as cyanobacteria, green and red algae, moss, and higher plants; however, a function has not yet been reported for any of these proteins. Therefore, DAC is a novel conserved protein that functions in the biogenesis of the Cyt b6/f complex.

In the *dac* mutant, the subunits of the Cyt b6/f complex were reduced to 10% to 15% of the wild-type levels (Fig. 3A; Supplemental Fig. S1), which was in accordance with the spectroscopic data indicating that the electron transport between PSI and PSII was blocked (Fig. 2). Additionally, the PSI and PSII complexes were functional despite a reduction in their protein levels. P700 absorbance kinetics and immunoblot analyses showed a more pronounced effect on PSI than PSII. A similar phenomenon has been observed in the *hcf208* mutant affecting the accumulation of native Cyt b_6 in Arabidopsis. One possibility is that this could be due to photooxidative damage of PSI. It is also possible that the perturbed photosynthetic redox control could lead to the down-regulation of expression of nucleus-encoded PSI proteins (Nott et al., 2006). However, the protein contents of PSI and PSII recovered to nearly wild-type levels when the *dac* mutants were cultivated under very low light (20 μmol m^{-2} s^{-1}; data not shown), indicating that the reduction of PSI and PSII is a secondary effect of the mutation, similar to what was reported for the *hcf164* mutant (Lennartz et al., 2001). Thus, the *dac* mutant is considered a mutant that is affected specifically in the Cyt b6/f complex. When grown in soil, homozygous *dac* plants die within 2 weeks. The *ccb* mutants, in which the levels of accumulated Cyt b_6 and Cyt *f* are dramatically reduced to 5% to 10% of wild-type values, also die as seedlings when grown on medium lacking a reduced carbon source (Lezhneva et al., 2008). The *hcf153* mutant retains approximately 25% of wild-type levels of the Cyt b6/f complex subunits and cannot grow photoautotrophically (Lennartz et al., 2006), whereas the *pgr3* mutant contains approximately 50% to 70% of wild-type levels of Cyt b6/f subunits and exhibits photoautotrophic growth rates similar to the wild-type plants under conditions of low light (40 μmol m^{-2} s^{-1}; Yamazaki et al., 2004). It is probable that the accumulation of a certain amount of the Cyt b6/f complex is critical for plant survival. In some mutants disrupted in the

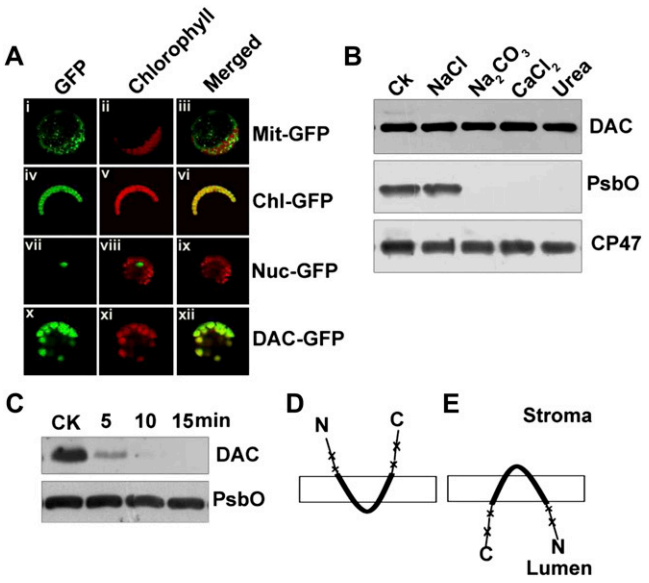

Figure 7. Subcellular localization and topology of the DAC protein. A, Subcellular localization of the DAC protein. The indicated sGFP fusion proteins were transiently expressed in Arabidopsis protoplasts under the control of the cauliflower mosaic virus 35S promoter, and the green GFP signals were monitored using confocal microscopy (panels i, iv, vii, and x). The chloroplasts were visualized by chlorophyll autofluorescence (panels ii, v, viii, and xi). The colocalization of GFP with the chloroplasts is indicated in the merged images (panels iii, vi, ix, and xii). The constructs used for transformation are indicated to the right: Nuc-GFP, control with the nuclear localization signal of fibrillarin; Mit-GFP, control with the mitochondrial localization signal of FRO1; Chl-GFP, control with the transit peptide of the ribulose bisphosphate carboxylase small subunit; DAC-GFP, the DAC-GFP fusion protein. B, Salt washing of the thylakoid membranes. Sonicated wild-type thylakoid membrane preparations were incubated with 1 M NaCl, 1 M $CaCl_2$, 200 mM Na_2CO_3, and 6 M urea for 30 min at 4°C. After this treatment, the membrane fractions were separated by Tricine/SDS-PAGE, followed by immunoblot analysis using anti-DAC, anti-PsbO, and anti-CP47 antibodies. Untreated sonicated membrane preparations (Ck) were used as controls. C, Protease protection experiment. Thylakoid membranes from wild-type leaves were incubated with trypsin for 0, 5, 10, and 15 min at 20°C, followed by immunoblot analysis using anti-DAC and anti-PsbO antibodies. D and E, Schematic representations of the two possible topologies of DAC. In contrast to the N and C termini, the loop between the two TM helices lacks predicted trypsin cleavage sites (indicated by asterisks). The antibody was produced against the C-terminal fragments (amino acids 147–190) of the DAC protein.

biogenesis of photosynthetic iron-sulfur clusters, the accumulation of the Cyt b6/f complex can be affected by the damage to the 2Fe-2S cluster incorporated into PetC (Lezhneva et al., 2004; Van Hoewyk et al., 2007). In the *dac* mutant, the 2Fe-2S protein Fd accumulated normally (Fig. 3A). Thus, it is unlikely that the reduction in the Cyt b6/f complex in the *dac* mutant is due to an involvement of DAC in the biogenesis of the iron-sulfur cluster affecting the accumulation of PetC.

The in vivo labeling of chloroplast proteins coupled with immunoprecipitation analysis demonstrated that the labeling rates of Cyt *f* and PetD in *dac* mutants were 30% to 40% of wild-type levels after 10 min of pulse labeling and were more than 80% lower after pulse labeling for 30 min (Fig. 4B). This result showed an increased labeling of Cyt *f*, Cyt b_6, and PetD after 10 min of pulse labeling compared with 30 min of pulse labeling (Fig. 4B). However, 10% to 15% of Cyt b6/f proteins accumulate in a stable manner (Fig. 5B). These results clearly indicated that a considerable part of the newly synthesized PetD, Cyt b_6, and Cyt *f* is rapidly degraded. The decreased labeling of PetD and Cyt *f* could be explained either by rapid degradation of the translation products and/or by a CES-like process involved in the coordination of protein stoichiometry of the cytochrome complex (Kuras and Wollman, 1994; Choquet et al., 1998). In *C. reinhardtii*, the synthesis of Cyt *f* has

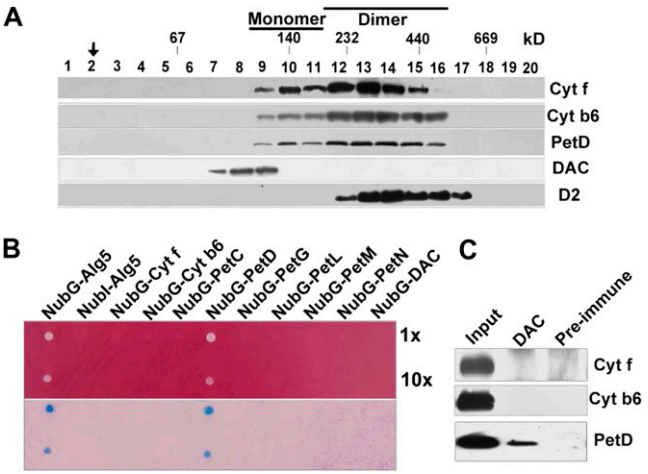

Figure 8. Suc gradient fractionation and protein interaction analysis. A, Thylakoid membranes from wild-type plants (0.5 mg mL^{-1}) were solubilized with 1% DM and separated in a linear 0.1 to 1 M Suc gradient. Twenty fractions were collected from the gradients, and the proteins from each fraction were separated by Tricine/SDS-PAGE. After electrophoresis, the separated proteins were immunodetected using anti-Cyt *f*, anti-Cyt b_6, anti-PetD, anti-DAC, and anti-D2 antibodies. The positions of the molecular size markers are indicated, as described previously (Peng et al., 2006). The position of the relative molecular mass of the DAC monomer is indicated by the arrow, and the positions of the monomer and dimer of Cyt b6/f are labeled. B, Split-ubiquitin-based yeast two-hybrid analysis. The full-length mature DAC protein fused to the LexA-VP16-Cub fragment of the pNCW vector was used as the bait. The full-length mature subunits of the Cyt b6/f complex fused to the NubG fragment of the pDSLNx vector were used as the prey. Alg5-NubI, a fusion of the unrelated endoplasmic reticulum membrane protein Alg5 to NubI (wild-type Nub), was used as a positive control. Negative controls were fusions of Alg5 to NubG (Alg5-NubG) as well as the empty vector expressing soluble NubG. C, Coimmunoprecipitation analysis. DM-solubilized thylakoid membranes from wild-type plants were incubated with protein A/G-agarose beads coupled to anti-DAC, anti-PetD, or anti-Cyt b_6 antibodies or preimmune serum (Preimmune). The precipitated proteins were separated by Tricine/SDS-PAGE, followed by immunoblot analysis. Input, DM-solubilized thylakoid membranes.

been shown to be regulated by the assembly state of Cyt b_6 or PetD, and the rates of synthesis of Cyt b_6 and PetD are independent (Kuras and Wollman, 1994). Thus, it is possible that a block in the assembly of PetD leads to a decrease in the synthesis and/or stability of Cyt *f*, especially considering the function of DAC in the assembly of PetD into the Cyt b6/f complex. The accumulation of unassembled Cyt *f* in the membrane down-regulates the initiation of translation of further *petA* transcripts through interactions with their 5′ untranslated regions in *C. reinhardtii* (Choquet et al., 1998). Analysis of the association of *petA* and *petD* transcripts with polysomes showed that the polysome association of these genes was not perturbed in the mutant (Fig. 4B). In addition, the labeling results showed increased degradation rates for Cyt *f*, Cyt b_6, and PetD in the *dac* mutant (Fig. 4B). Thus, it is likely that the reduced labeling rate of proteins in the mutant would be due to a rapid degradation of newly synthesized proteins that cannot be assembled efficiently into complexes (Fig. 5A). Such assembly-dependent regulatory processes have been reported in the biogenesis of PSII: rapid degradation of corresponding subunits of PSII in the absence of LPA1 and LPA2 occurs with no changes in polysome loading (Peng et al., 2006; Ma et al., 2007).

The amount of radioactivity incorporated into Cyt b_6 was higher in the *dac* mutant than in the wild-type plants after pulse labeling (Fig. 4B). In consideration of the amounts of stably accumulated Cyt b_6 (10%–15%) in the mutant (Fig. 3A), the high synthesis rates of Cyt b_6 after 10 min of pulse labeling highlights the strong reduction of Cyt b_6 in the mutant. It is very likely that the low Cyt b_6 protein level in the *dac* mutant is the result of increased protein degradation. Thus, the 10% to 15% of Cyt b_6 accumulated in the mutant (Fig. 3A) could escape degradation and be processed normally (Fig. 3A). A similar phenomenon has been observed in the *crp1* mutant (Barkan et al., 1994). In *crp1*, the synthesis of Cyt *f* and PetD was reduced greatly, while Cyt b_6 was synthesized normally after pulse labeling for 20 min, and the Cyt *f*, Cyt b_6, and PetD proteins accumulated to less than 5% of wild-type levels. Increased labeling of Cyt b_6 in the *crp1* mutant compared with wild-type plants was observed when the labeling time was shortened to 5 min.

Using BN-PAGE analysis, the monomer and dimer of Cyt b6/f could be observed in the mutant samples when a much longer exposure time was used (Fig. 3C). This indicates that the subunits of the Cyt b6/f complex can still assemble into monomer and dimer complexes despite a major reduction in their contents in the mutant. Relative to the monomer and dimer of the Cyt b6/f complex, an increase in a complex of approximately 90 kD was observed using BN-PAGE analysis (Fig. 3C). The molecular mass of this complex is larger than that of Cyt b_6 or PetD; although its identity remains unknown, this subcomplex may represent an assembly intermediate or a degradation product of the Cyt b6/f complex. Our immunoblot analyses showed that the subunits in the *dac* mutants are as stable as those in the wild-type plants (Fig. 5B), suggesting that DAC may be involved in the assembly of the Cyt b6/f complex. The intermediate may be formed by the subunits of the Cyt b6/f complex; for example, PetD and Cyt b_6 may form a subcomplex or interact with assembly factors. Taken together, these data indicate that the efficiency of subunit assembly is very likely to be affected in the *dac* mutants and may be responsible for the reduced accumulation of the Cyt b6/f complex. The subcomplex detected during BN-PAGE analysis may also be a destabilized product of the Cyt b6/f complex during gel electrophoresis. The ratio between the monomer and dimer is lower in the *dac* mutant than in the wild-type plants, which may suggest a decreased stability of the Cyt b6/f monomer in *dac* mutants (Fig. 3C). A possible function of DAC in the accumulation of stable monomer cannot be excluded.

DAC was not found to comigrate with the Cyt b6/f complex (Fig. 8A), indicating that it is not a component of the complex, which is consistent with structural and biochemical studies (Mosser et al., 1997). The molecular mass of mature DAC is expected to be approximately 16 kD (Fig. 1D), but a signal for DAC after Suc gradient fractionation was identified with a mass of approximately 80 to 100 kD (Fig. 8A), which partially overlaps with the Cyt *f*, Cyt b_6, and PetD subunits. This finding indicates that DAC was present in an oligomeric form or was potentially associated with the subunits of the Cyt b6/f complex. Our yeast two-hybrid and coimmunoprecipitation analyses revealed that DAC interacts with PetD but not with the Cyt *f* and Cyt b_6 subunits. Previous studies have revealed that the physical interaction of assembly factors with specific PSII subunits is important for assembly (Peng et al., 2006; Ma et al., 2007; Armbruster et al., 2010). In addition, studies on the import and assembly of the Cyt b6/f complex in isolated pea (*Pisum sativum*) chloroplasts suggested the presence of unassembled subunits available for assembly (Mould et al., 2001). Thus, it is reasonable to speculate that DAC may interact with PetD before PetD is assembled into a complex and that, when PetD assembly occurs, the interaction between DAC and PetD is lost, and thus DAC is no longer present in the Cyt b6/f complex. Similar observations have been reported in studies of the functions of the CCB proteins in heme incorporation, in which the results were explained by the fact that the interaction between the CCBs and Cyt b_6 occurs before Cyt b_6 assembly within the Cyt b6/f complex (Saint-Marcoux et al., 2009). The specificity of the interaction between DAC and PetD suggests that DAC may function in the assembly/stabilization of PetD.

MATERIALS AND METHODS

Plant Materials and Growth Conditions

The Arabidopsis (*Arabidopsis thaliana*) *dac* mutant (SALK_088638; ecotype Columbia) was obtained from the Arabidopsis Biological Resource Center. The

T-DNA was inserted into exon 4 of *AT3G17930*, and the homozygous mutant was confirmed by PCR using primers LP (5′-GTAAGGCATTTGGGTGAGAG-3′) and RP (5′-TCGTCGTAGTAGTCCTGAAG-3′). The T-DNA insertion was verified by PCR followed by sequencing using primers LB (5′-ATTTTGCCGATTTCGGAAC-3′) and RP. For complementation of the *dac* mutant, the coding region was amplified with primers 5′-GGATCCATGGCTTCTTTACCGTTC-3′ and 5′-GAGCTCCTACTCAACCTTGGTCTTC-3′. The PCR product was cleaved with *Bam*HI and *Sac*I and then subcloned into the plant expression vector pSN1301 under the control of the cauliflower mosaic virus 35S promoter. The construct was transformed into *Agrobacterium tumefaciens* EHA105 strain and introduced into heterozygous *dac* plants by the floral dip method (Clough and Bent, 1998). Transgenic plants were selected on Murashige and Skoog medium containing 50 mg L^{-1} hygromycin, and successful complementation was confirmed by PCR and chlorophyll fluorescence analysis.

The *dac* mutant and wild-type plants were grown on Murashige and Skoog (1962) medium containing 3% Suc and 0.8% agar at 22°C with a photon flux density of 50 μmol m^{-2} s^{-1} in a photoperiod of 10 h of light and 14 h of darkness.

Chlorophyll Fluorescence and P700 Absorbance Measurements

The chlorophyll fluorescence measurements were conducted using a portable chlorophyll fluorometer (PAM-2000; Walz) connected to a leaf-clip holder (model 2030-B; Walz). Before measurement, leaves were dark adapted for 30 min. The minimum fluorescence yield (F_o) was measured under measuring light with very low intensity (0.8 μmol m^{-2} s^{-1}). To estimate the maximum fluorescence yield (F_m), a saturating pulse of white light (3,000 μmol m^{-2} s^{-1} for 1 s) was applied. The leaf was illuminated with actinic light at an intensity of 50 μmol m^{-2} s^{-1} to drive electron transport between PSII and PSI. After about 5 to 6 min, photosynthesis reached steady-state conditions and the steady-state fluorescence (F_s) was recorded. After exposure to another saturation pulse (3,000 μmol m^{-2} s^{-1} for 1 s), F_m' was determined. The minimal fluorescence F_o' was obtained by switching off the actinic light in the light-adapted state. The fraction of the PSII reaction centers remaining in the open state under continuous illumination $[(F_m' - F_s)/(F_m' - F_o')] \times (F_o'/F_s)]$ was calculated according to Kramer et al. (2004). The measurement of light-induced P700 was performed using a PAM101 fluorometer connected to a dual-wavelength emitter unit (ED-P800T; Walz) according to Peng et al. (2006). Plants were illuminated with actinic light (50 μmol m^{-2} s^{-1}), which was switched off to measure the oxidation of P700 under actinic light. Then, switching far-red light on was applied to selectively oxidize PSI. Maximum oxidation induced by far-red light was attained under a background of far-red light. The spectroscopic analyses were normalized based on leaf area. The values are means ± SD of five independent experiments.

Thylakoid Membrane and Total Protein Preparations

Thylakoid membranes were prepared as described previously by Ma et al. (2007). The leaves were homogenized on ice in 400 mM Suc, 50 mM HEPES-KOH (pH 7.8), 10 mM NaCl, and 2 mM $MgCl_2$ and filtered through two layers of cheesecloth. The resulting filtrates were centrifuged at 5,000*g* for 10 min at 4°C, and the thylakoid pellets were resuspended in the homogenization buffer. The total proteins were extracted from 4-week-old Arabidopsis leaves, and the protein concentrations were determined using the Bio-Rad detergent-compatible colorimetric protein assay.

BN-SDS-PAGE, Immunoblot Analysis, and Heme Staining

The BN-PAGE was performed essentially according to Schägger et al. (1994), with the modifications described by Peng et al. (2006). For the two-dimensional analysis, the excised BN-PAGE lanes were soaked for 30 min in SDS sample buffer supplemented with 5% β-mercaptoethanol prior to SDS-PAGE. Tricine/SDS-PAGE was performed according to Schägger and von Jagow (1987). After electrophoresis, the proteins resolved by SDS-PAGE were transferred to nitrocellulose membranes and incubated with specific antibodies, and the signals were visualized using the enhanced chemiluminescence method. Aliquots of 15 μg (wild type), 7.5 μg (one-half wild type), 3.75 μg (one-quarter wild type), and 15 μg (*dac*) of total protein were loaded. For the detection of heme peroxidase activity, aliquots of 25 μg (wild type), 12.5 μg (one-half wild type), 6.25 μg (one-quarter wild type), and 25 μg (*dac*) of chlorophyll of thylakoid membranes were loaded. The proteins were blotted onto nitrocellulose membranes, incubated with the reagent of the assay (ECL Plus; GE Healthcare), and exposed to x-ray film for 0 to 30 min. M_r standard was according to the prestained protein marker P7708 (New England Biolabs).

Nucleic Acid Preparation and Analysis

Total plant RNA was extracted from 100 mg of fresh tissues using Trizol reagent. RNA gel-blot analysis was performed essentially as described before (Chi et al., 2012). After gel electrophoresis with a formaldehyde denaturing 1.2% agarose gel, total RNA was transferred onto nylon membranes (Amersham Pharmacia Biotech). The membranes were probed with ^{32}P-labeled complementary DNA (cDNA) probes. Following high-stringency hybridization and washing, all the blots were exposed to x-ray film for 1 to 2 d. The hybridization probes of *petA*, *petB*, *petC*, *petD*, *petB/D*, and *petM* were labeled by random priming and prepared from the PCR fragments of the chloroplast genome. The hybridization probes of *petL*, *petG*, and *petN* were prepared by PCR methods with specific primers. The sequences of the PCR primers used for the amplification of chloroplast genes are given in Supplemental Table S1. Polysomes were isolated from leaf tissues under conditions that maintain polysome integrity according to Barkan (1988). RNA was isolated, fractionated, and transferred onto nylon membranes and next used in RNA gel-blot analysis.

In Vivo Labeling of Chloroplast Proteins and Immunoprecipitation Assay

Primary leaves of 15-d-old plants with equal weight were preincubated in 20 μg mL^{-1} cycloheximide for 30 min followed by radiolabeling with 1 μCi μL^{-1} [^{35}S] Met (specific activity > 1,000 Ci $mmol^{-1}$) in the presence of 20 μg mL^{-1} cycloheximide for 10 min and 30 min at 22°C. The thylakoid membranes were isolated after washing twice with homogenization buffer (50 mM Tris-HCl [pH 7.5], 150 mM NaCl, and 2 mM EDTA). The equal amounts of thylakoid membrane protein were confirmed by Coomassie blue staining. For the immunoprecipitation, aliquots equivalent to 200,000 cpm of the incorporated label were diluted 10-fold with 50 mM Tris-HCl (pH 7.5), 150 mM NaCl, 2 mM EDTA, and 1% (v/v) Nonidet P-40 and incubated with 50 μL of specific antibody at 4°C for 2 h. Subsequently, 30 μL of protein A/G-agarose (Abmart) was added, and the incubation was continued overnight. The agarose beads were washed four times with 50 mM Tris-HCl (pH 7.5), 150 mM NaCl, 2 mM EDTA, and 1% (v/v) Nonidet P-40, and the precipitated proteins were dissociated in SDS sample buffer at 70°C for 10 min. To ensure the quantitative precipitation of the proteins, the supernatants collected after the first immunoprecipitation were incubated with the same amount of antibody. The precipitated proteins were subjected to Tricine/SDS-PAGE and visualized using autoradiography.

Stability of Thylakoid Membrane Proteins

Arabidopsis leaves collected from 4-week-old plants were incubated for 30 min (Sun et al., 2007) in the presence of 100 μg mL^{-1} lincomycin, which block the synthesis of plastid-encoded proteins. The leaves were subsequently illuminated at a fluence of 50 μmol m^{-2} s^{-1} for 0, 2, 4, 6, and 8 h. After treatment, the thylakoid membranes were isolated, and the contents of the chloroplast proteins were examined using immunoblot analysis.

Antiserum Production

The nucleotide sequences encoding the soluble part of DAC (amino acids 147–190, corresponding to nucleotide positions 439–570 in the *DAC* gene) were amplified by PCR using primers DAC-F, 5′-AGGAATTCGAGATGACTTATGCCCA-3′, and DAC-R, 5′-CAGTCGACCTCAACCTTGGTCTTCT-3′. The resulting DNA fragment was cleaved with *Eco*RI and *Sal*I and fused in frame with the C-terminal His affinity tag of pET28a. The antigen was purified, and polyclonal antibodies were raised in a rabbit. The Cyt b_6 and PetD antibodies were raised against synthetic peptides corresponding to the C terminus of Cyt b_6 (FLMIRKQGISGP) and the C terminus of PetD (LPIDKSLTLGLF), respectively. The PetC antibody was purchased from Agrisera (no. As08330). Antibodies were raised in rabbits against D1, PsbO, PsaA/B, and CF1β purified from *Escherichia coli* strains expressing according to Meurer et al. (1996). PsaN antibody was raised against amino acids 90 to 165 and Fd antibody against amino acids 70 to 148 of their respective proteins. Antibody dilutions were 1:2,000 for anti-DAC, anti-PetC, anti-D1, anti-PsaA/B, and anti-PsaN and 1:3,000 for anti-Cyt b6, anti-PetD, anti-PsbO, anti-Cf1β, and anti-Fd. A 1:10,000 dilution of alkaline phosphatase-conjugated goat anti-rabbit IgG was used as the secondary antibody.

Subcellular Localization of GFP Proteins

The open reading frame of the DAC protein was amplified by PCR using primers DACGFP-F, 5′-GTCGACATGGCTTCTTTACCGTTC-3′, and DACGFP-R, 5′-CCATGGACTCAACCTTGGTCTTCTC-3′. The PCR products were digested with *Sal*I and *Nco*I and cloned into the GFP fusion vector, pUC18-35s-sGFP. The vectors for nuclear, chloroplast, and mitochondrial localization were constructed according to Cai et al. (2009). The resulting fusion constructs and the control vector were introduced into wild-type Arabidopsis. The GFP signals in the examined samples were visualized using a confocal laser-scanning microscope (LSM510; Carl Zeiss).

Immunolocalization Studies

The localization of the DAC proteins was examined according to Sun et al. (2007). For the protease protection assay, trypsin was added to Arabidopsis thylakoid membranes (0.1 mg chlorophyll mL^{-1}) to a final concentration of 20 μg mL^{-1} and incubated at 25°C. For the salt washing assay, the thylakoid membranes were incubated with 1 M NaCl, 1 M $CaCl_2$, 200 mM Na_2CO_3, and 6 M urea for 30 min at 4°C. After the treatment, the thylakoid membranes were solubilized in SDS sample buffer, and the proteins were separated by Tricine/SDS-PAGE and immunodetected with specific antibodies.

Suc Gradient Fractionation of Thylakoid Membranes

Arabidopsis thylakoid membranes (0.5 mg chlorophyll mL^{-1}) were solubilized for 5 min on ice in 5 mM $MgCl_2$, 10 mM NaCl, and 25 mM MES-NaOH (pH 6.0) containing 1% DM. After centrifugation at 14,000*g* for 10 min at 4°C, the supernatant (500 μL) was loaded onto a linear 0.1 to 1 M Suc gradient in 5 mM $MgCl_2$, 10 mM NaCl, 0.06% DM, and 25 mM MES-NaOH (pH 5.7). The gradient was centrifuged for 22 h at 180,000*g* at 48°C using an SW40 Ti rotor (Beckman), and 20 fractions were collected from the top to the bottom of the gradient. After fractionation, the proteins in each fraction were separated by Tricine/SDS-PAGE, followed by immunoblot analysis. The M_r estimation of the localized proteins is described by Peng et al. (2006).

Protein Interaction Assays

For the coimmunoprecipitation analysis, thylakoid membranes were solubilized with 0.5% DM. After centrifugation at 14,000*g* for 15 min, the solubilized thylakoid membranes were incubated with anti-DAC antibody for 2 h at 4°C and then incubated with protein A/G-agarose (Abmart) overnight. The precipitated proteins were dissociated in SDS buffer at 70°C for 5 min and subjected to immunoblot analysis with specific antibodies.

The yeast (*Saccharomyces cerevisiae*) two-hybrid assay was performed following the protocols described by Dualsystems Biotech (Stagljar et al., 1998). The mature full-length DAC gene was cloned into the bait vector, pNCW, which encodes the LexA-VP16-Cub fragment. The mature full-length genes of the Cyt b6/f subunits were cloned into the prey vector, pDSLNx, which encodes the NubG fragment (Dualsystems Biotech). Interaction was determined by the growth of diploid yeast colonies on SD-His-Leu-Trp-Ade medium and also by β-galactosidase activity using the 5-bromo-4-chloro-3-indolyl-β-D-galactopyranoside filter assay (Stagljar et al., 1998).

Sequence data from this article can be found in the GenBank/EMBL data libraries under accession number DAC (At3g17930).

Supplemental Data

The following materials are available in the online version of this article.

Supplemental Figure S1. Semiquantitative analysis of chloroplast proteins.

Supplemental Table S1. Oligonucleotides used for the preparation of the hybridization probes.

Supplemental Table S2. Quantitative data on P700 oxidation.

ACKNOWLEDGMENTS

We thank the Arabidopsis Biological Resource Center for the *dac* mutant lines.

Received August 3, 2012; accepted October 4, 2012; published October 5, 2012.

LITERATURE CITED

Armbruster U, Zühlke J, Rengstl B, Kreller R, Makarenko E, Rühle T, Schünemann D, Jahns P, Weisshaar B, Nickelsen J, et al (2010) The *Arabidopsis* thylakoid protein PAM68 is required for efficient D1 biogenesis and photosystem II assembly. Plant Cell **22:** 3439–3460

Baniulis D, Yamashita E, Whitelegge JP, Zatsman AI, Hendrich MP, Hasan SS, Ryan CM, Cramer WA (2009) Structure-function, stability, and chemical modification of the cyanobacterial cytochrome b6f complex from *Nostoc* sp. PCC 7120. J Biol Chem **284:** 9861–9869

Barkan A (1988) Proteins encoded by a complex chloroplast transcription unit are each translated from both monocistronic and polycistronic mRNAs. EMBO J **7:** 2637–2644

Barkan A, Walker M, Nolasco M, Johnson D (1994) A nuclear mutation in maize blocks the processing and translation of several chloroplast mRNAs and provides evidence for the differential translation of alternative mRNA forms. EMBO J **13:** 3170–3181

Bendall DS, Sanguansermsri M, Girard-Bascou J, Bennoun P (1986) Mutations in *Chlamydomonas reinhardtii* affecting the cytochrome bf complex. FEBS Lett **203:** 31–35

Boulouis A, Raynaud C, Bujaldon S, Aznar A, Wollman FA, Choquet Y (2011) The nucleus-encoded trans-acting factor MCA1 plays a critical role in the regulation of cytochrome f synthesis in *Chlamydomonas* chloroplasts. Plant Cell **23:** 333–349

Breyton C, Tribet C, Olive J, Dubacq JP, Popot JL (1997) Dimer to monomer conversion of the cytochrome b6f complex: causes and consequences. J Biol Chem **272:** 21892–21900

Bruce BD, Malkin R (1991) Biosynthesis of the chloroplast cytochrome b6f complex: studies in a photosynthetic mutant of *Lemna*. Plant Cell **3:** 203–212

Cai W, Ji D, Peng L, Guo J, Ma J, Zou M, Lu C, Zhang L (2009) LPA66 is required for editing *psbF* chloroplast transcripts in Arabidopsis. Plant Physiol **150:** 1260–1271

Chi W, He B, Mao J, Li Q, Ma J, Ji D, Zou M, Zhang L (2012) The function of RH22, a DEAD RNA helicase, in the biogenesis of the 50S ribosomal subunits of Arabidopsis chloroplasts. Plant Physiol **158:** 693–707

Choquet Y, Stern DB, Wostrikoff K, Kuras R, Girard-Bascou J, Wollman FA (1998) Translation of cytochrome f is autoregulated through the 5′ untranslated region of petA mRNA in *Chlamydomona*s chloroplasts. Proc Natl Acad Sci USA **95:** 4380–4385

Choquet Y, Vallon O (2000) Synthesis, assembly and degradation of thylakoid membrane proteins. Biochimie **82:** 615–634

Choquet Y, Wostrikoff K, Rimbault B, Zito F, Girard-Bascou J, Drapier D, Wollman FA (2001) Assembly-controlled regulation of chloroplast gene translation. Biochem Soc Trans **29:** 421–426

Clough SJ, Bent AF (1998) Floral dip: a simplified method for Agrobacterium-mediated transformation of *Arabidopsis thaliana*. Plant J **16:** 735–743

de Vitry C (2011) Cytochrome c maturation system on the negative side of bioenergetic membranes: CCB or system IV. FEBS J **278:** 4189–4197

Friso G, Giacomelli L, Ytterberg AJ, Peltier JB, Rudella A, Sun Q, Wijk KJ (2004) In-depth analysis of the thylakoid membrane proteome of *Arabidopsis thaliana* chloroplasts: new proteins, new functions, and a plastid proteome database. Plant Cell **16:** 478–499

Huang D, Everly RM, Cheng RH, Heymann JB, Schägger H, Sled V, Ohnishi T, Baker TS, Cramer WA (1994) Characterization of the chloroplast cytochrome b6f complex as a structural and functional dimer. Biochemistry **33:** 4401–4409

Kramer DM, Johnson G, Kiirats O, Edwards GE (2004) New fluorescence parameters for the determination of q(a) redox state and excitation energy fluxes. Photosynth Res **79:** 209–218

Kuras R, de Vitry C, Choquet Y, Girard-Bascou J, Culler D, Büschlen S, Merchant S, Wollman FA (1997) Molecular genetic identification of a pathway for heme binding to cytochrome b6. J Biol Chem **272:** 32427–32435

Kuras R, Saint-Marcoux D, Wollman FA, de Vitry C (2007) A specific c-type cytochrome maturation system is required for oxygenic photosynthesis. Proc Natl Acad Sci USA **104:** 9906–9910

Kuras R, Wollman FA (1994) The assembly of cytochrome b6/f complexes: an approach using genetic transformation of the green alga *Chlamydomonas reinhardtii*. EMBO J **13:** 1019–1027

Lemaire C, Girard-Bascou J, Wollman F-A, Bennoun P (1986) Studies on the cytochrome b6f complex. I. Characterization of the complex subunits in Chlamydomonas reinhardtii. Biochim Biophys Acta **851:** 229–238

Lennartz K, Bossmann S, Westhoff P, Bechtold N, Meierhoff K (2006) HCF153, a novel nuclear-encoded factor necessary during a post-translational step in biogenesis of the cytochrome bf complex. Plant J **45:** 101–112

Lennartz K, Plücken H, Seidler A, Westhoff P, Bechtold N, Meierhoff K (2001) *HCF164* encodes a thioredoxin-like protein involved in the biogenesis of the cytochrome b_6f complex in *Arabidopsis*. Plant Cell **13:** 2539–2551

Lezhneva L, Amann K, Meurer J (2004) The universally conserved HCF101 protein is involved in assembly of [4Fe-4S]-cluster-containing complexes in Arabidopsis thaliana chloroplasts. Plant J **37:** 174–185

Lezhneva L, Kuras R, Ephritikhine G, de Vitry C (2008) A novel pathway of cytochrome c biogenesis is involved in the assembly of the cytochrome b6f complex in Arabidopsis chloroplasts. J Biol Chem **283**: 24608–24616

Lyska D, Paradies S, Meierhoff K, Westhoff P (2007) HCF208, a homolog of *Chlamydomonas* CCB2, is required for accumulation of native cytochrome b6 in *Arabidopsis thaliana*. Plant Cell Physiol **48:** 1737–1746

Ma J, Peng L, Guo J, Lu Q, Lu C, Zhang L (2007) LPA2 is required for efficient assembly of photosystem II in *Arabidopsis thaliana*. Plant Cell **19:** 1980–1993

Maiwald D, Dietzmann A, Jahns P, Pesaresi P, Joliot P, Joliot A, Levin JZ, Salamini F, Leister D (2003) Knock-out of the genes coding for the Rieske protein and the ATP-synthase delta-subunit of Arabidopsis: effects on photosynthesis, thylakoid protein composition, and nuclear chloroplast gene expression. Plant Physiol **133:** 191–202

Meierhoff K, Felder S, Nakamura T, Bechtold N, Schuster G (2003) HCF152, an *Arabidopsis* RNA binding pentatricopeptide repeat protein involved in the processing of chloroplast psbB-psbT-psbH-petB-petD RNAs. Plant Cell **15:** 1480–1495

Meurer J, Meierhoff K, Westhoff P (1996) Isolation of high-chlorophyll-fluorescence mutants of *Arabidopsis thaliana* and their characterisation by spectroscopy, immunoblotting and northern hybridisation. Planta **198:** 385–396

Mitchell P (1961) Coupling of phosphorylation to electron and hydrogen transfer by a chemi-osmotic type of mechanism. Nature **191:** 144–148

Mosser G, Breyton C, Olofsson A, Popot JL, Rigaud JL (1997) Projection map of cytochrome b6f complex at 8 A resolution. J Biol Chem **272:** 20263–20268

Mould RM, Kapazoglou A, Gray JC (2001) Assembly of cytochrome f into the cytochrome bf complex in isolated pea chloroplasts. Eur J Biochem **268:** 792–799

Mulo P, Sirpiö S, Suorsa M, Aro EM (2008) Auxiliary proteins involved in the assembly and sustenance of photosystem II. Photosynth Res **98:** 489–501

Murashige T, Skoog F (1962) A revised medium for rapid growth and bioassays with tobacco tissue cultures. Physiol Plant **15:** 473–497

Nakamoto SS, Hamel P, Merchant S (2000) Assembly of chloroplast cytochromes b and c. Biochimie **82:** 603–614

Nixon PJ, Michoux F, Yu J, Boehm M, Komenda J (2010) Recent advances in understanding the assembly and repair of photosystem II. Ann Bot (Lond) **106:** 1–16

Nott A, Jung HS, Koussevitzky S, Chory J (2006) Plastid-to-nucleus retrograde signaling. Annu Rev Plant Biol **57:** 739–759

Ouyang M, Li X, Ma J, Chi W, Xiao J, Zou M, Chen F, Lu C, Zhang L (2011) LTD is a protein required for sorting light-harvesting chlorophyll-binding proteins to the chloroplast SRP pathway. Nat Commun **2:** 277–285

Peltier JB, Emanuelsson O, Kalume DE, Ytterberg J, Friso G, Rudella A, Liberles DA, Söderberg L, Roepstorff P, von Heijne G, et al (2002) Central functions of the lumenal and peripheral thylakoid proteome of *Arabidopsis* determined by experimentation and genome-wide prediction. Plant Cell **14:** 211–236

Peng L, Ma J, Chi W, Guo J, Zhu S, Lu Q, Lu C, Zhang L (2006) LOW PSII ACCUMULATION1 is involved in efficient assembly of photosystem II in *Arabidopsis thaliana*. Plant Cell **18:** 955–969

Rochaix JD (2011) Assembly of the photosynthetic apparatus. Plant Physiol **155:** 1493–1500

Saint-Marcoux D, Wollman FA, de Vitry C (2009) Biogenesis of cytochrome b6 in photosynthetic membranes. J Cell Biol **185:** 1195–1207

Saraste M (1999) Oxidative phosphorylation at the fin de siècle. Science **283:** 1488–1493

Schägger H, Cramer WA, von Jagow G (1994) Analysis of molecular masses and oligomeric states of protein complexes by blue native electrophoresis and isolation of membrane protein complexes by two-dimensional native electrophoresis. Anal Biochem **217:** 220–230

Schägger H, von Jagow G (1987) Tricine-sodium dodecyl sulfate-polyacrylamide gel electrophoresis for the separation of proteins in the range from 1 to 100 kDa. Anal Biochem **166:** 368–379

Schneider D, Berry S, Rich P, Seidler A, Rögner M (2001) A regulatory role of the PetM subunit in a cyanobacterial cytochrome b6f complex. J Biol Chem **276:** 16780–16785

Schwenkert S, Legen J, Takami T, Shikanai T, Herrmann RG, Meurer J (2007) Role of the low-molecular-weight subunits PetL, PetG, and PetN in assembly, stability, and dimerization of the cytochrome b6f complex in tobacco. Plant Physiol **144:** 1924–1935

Stagljar I, Korostensky C, Johnsson N, te Heesen S (1998) A genetic system based on split-ubiquitin for the analysis of interactions between membrane proteins *in vivo*. Proc Natl Acad Sci USA **95:** 5187–5192

Sun X, Peng L, Guo J, Chi W, Ma J, Lu C, Zhang L (2007) Formation of DEG5 and DEG8 complexes and their involvement in the degradation of photodamaged photosystem II reaction center D1 protein in *Arabidopsis*. Plant Cell **19:** 1347–1361

Van Hoewyk D, Abdel-Ghany SE, Cohu CM, Herbert SK, Kugrens P, Pilon M, Pilon-Smits EA (2007) Chloroplast iron-sulfur cluster protein maturation requires the essential cysteine desulfurase CpNifS. Proc Natl Acad Sci USA **104:** 5686–5691

Wollman FA (2004) The structure, function and biogenesis of cytochrome b6f complexes. Adv Photosynth Res **7:** 459–476

Xie Z, Merchant S (1998) A novel pathway for cytochromes c biogenesis in chloroplasts. Biochim Biophys Acta **1365:** 309–318

Yamazaki H, Tasaka M, Shikanai T (2004) PPR motifs of the nucleus-encoded factor, PGR3, function in the selective and distinct steps of chloroplast gene expression in *Arabidopsis*. Plant J **38:** 152–163

Zhang H, Whitelegge JP, Cramer WA (2001) Ferredoxin:NADP+ oxidoreductase is a subunit of the chloroplast cytochrome b6f complex. J Biol Chem **276:** 38159–38165